SCIENTIFIC REPORTS

OPEN

SUBJECT AREAS:
MAGNETIC PROPERTIES AND MATERIALS
NANOSCALE MATERIALS

Received
10 July 2013

Accepted
16 August 2013

Published
6 September 2013

Correspondence and requests for materials should be addressed to L.G. (lwguo@iphy.ac.cn) or X.C. (xlchen@iphy.ac.cn)

Towards intrinsic magnetism of graphene sheets with irregular zigzag edges

Lianlian Chen, Liwei Guo, Zhilin Li, Han Zhang, Jingjing Lin, Jiao Huang, Shifeng Jin & Xiaolong Chen

Research & Development Center for Functional Crystals, Beijing National Laboratory for Condensed Matter Physics, Institute of Physics, Chinese Academy of Sciences, P.O. Box 603, Beijing 100190, China.

The magnetism of graphene has remained divergent and controversial due to absence of reliable experimental results. Here we show the intrinsic magnetism of graphene edge states revealed based on unidirectional aligned graphene sheets derived from completely carbonized SiC crystals. It is found that ferromagnetism, antiferromagnetism and diamagnetism along with a probable superconductivity exist in the graphene with irregular zigzag edges. A phase diagram is constructed to show the evolution of the magnetism. The ferromagnetic ordering curie-temperature of the fundamental magnetic order unit (FMOU) is 820 ± 80 K. The antiferromagnetic ordering Neel temperature of the FMOUs belonging to different sublattices is about 54 ± 2 K. The diamagnetism is similar to that of graphite and can be well described by the Kotosonov's equation. Our experimental results provide new evidences to clarify the controversial experimental phenomena observed in graphene and contribute to a deeper insight into the nature of magnetism in graphene based system.

Exploring intrinsic magnetism of graphene has been a long standing interest for realizing application of graphene in spintronic[1]. Magnetic response in graphene by introduction of edges, vacancy defects or adatoms has intriguing much theoretical and experimental investigation[1–13], since this would play a significant role in novel spintronic devices by combining advantages of charge and spin[1–4]. So far there have been many theoretical studies[3–10] suggested that zigzag edges or point defects in graphene as the spin units should carry magnetic moments and the possible long-range order coupling among them is in principle ferromagnetic or antiferromagnetic, depending on whether the zigzag edges or defects correspond to the same or to different hexagonal sublattice of the graphene lattice, respectively. Usually, as-grown graphene single crystalline sheet is finite in size and shape. While its size approaches to nanometric or micrometric dimensions, its geometrical shape becomes extremely importance because its edges are composed of a combination of armchair and zigzag edges, that had been predicted possessing spin-polarized electron state (edge-state) localized in the zigzag edge region in spite of the absence of such state in armchair edges[8]. However, experimental evidence from a graphene for such magnetism remains both scarce and controversial[2,10–13]. Room temperature (RT) ferromagnetism (FM)[10–12], a weak paramagnetic (PM)[2,13] and even a RT superconductivity from a water-treated graphite powder had been reported[14]. These divergent and controversial experimental results are ascribed to adopted graphene samples are not a massive amount of high-purity graphene as pointed out by Nair et al[2]. At present, the intrinsic magnetic properties of graphene in finite sizes are far from being understood, because magnetic signal from one piece of graphene in finite size is too weak to be detected by macro-magnetic measurement. Therefore, a massive amount of high-purity graphene (at least in milligram-scale) is an essential prerequisite to unveil the intrinsic magnetism contributed from graphene edges or vacancy defects.

Fortunately, fabrication of the graphene by thermal decomposition of SiC is a mature method and the prepared graphene had been widely used for graphene-based high frequency devices[15]. Further development of the method for the massive graphene sheets had been reported[16,17]. Through carbonizing SiC (10-10) slice completely, a massive amount of high-purity graphene assemblage with unidirectional aligned graphene basal planes (GBPs) was obtained, which provides possibility to measure anisotropic macroscopic magnetism of graphene. Therefore, the unusual magnetism of graphene with irregular zigzag edges is unveiled thoroughly, that is a coexisting of ferromagnetism (FM), antiferromagnetism (AFM) and diamagnetism (DM) together with a probable superconductivity. Furthermore, a magnetic phase diagram was constructed unambiguously for the first time under a frame of magnetic field and temperature, which is significant to understand magnetic ordering phenomenon observed here intuitively and contribute a deeper insight into the nature of magnetism in graphene based system.

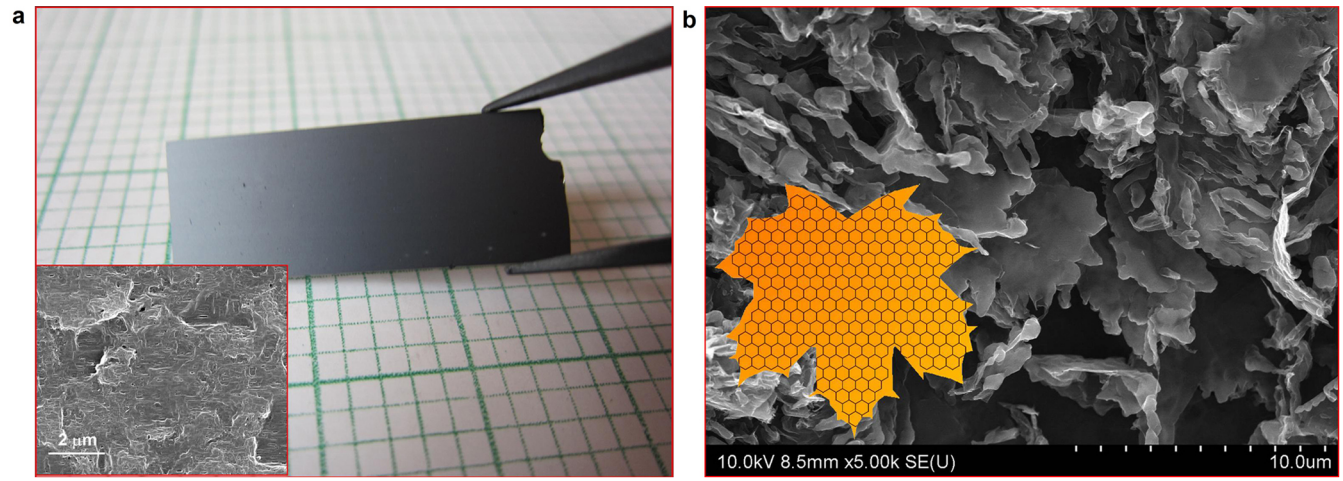

Figure 1 | Optical and cross-sectional SEM images of the completely carbonized graphene sample derived from SiC in Fig. 1a and 1b, respectively. The inset in Fig. 1a is a top view SEM image of the sample and the inset in Fig. 1b is a maple leaf picture together with a schematic a piece of graphene sheet for comparison.

Results

Figure 1**a** and 1**b** are optical and cross-sectional scanning electron microscopy (SEM) images, respectively, of the completely carbonized graphene sample. It is noted the shape of the large size graphene sheets in Fig. 1**b** is like maple leaves as shown in the inset of Fig. 1**b**, whose periphery shows near regular geometry similar to what observed in graphene grown by chemical vapor deposition (CVD)[18,19]. It is this kind of graphene boundary composed of the zigzag edge dominated domains renders the graphene sheets unusual magnetic properties.

The M(T)/H curves (normalized with the applied field) with the field parallel and perpendicular to the GBPs under the fields 1 and 3 kOe at field cooling (FC) and zero field cooling (ZFC) are shown in Fig. 2**a** and 2**b** respectively. The M(T)/H curves exhibit DM response over the whole temperature range, whose temperature coefficient is similar to what observed in graphite[20,21]. The DM susceptibility has been ascribed to the contribution of the free electrons due to the quantized orbital motions of electrons in a magnetic field[22,23]. It is noted that a sharp peak located at about 52–56 K is overlapped on the background of the DM, which became even prominent under a 1 kOe field parallel to the GBPs as seen in Fig. 2**a**. Its shape and intensity did not vary no matter it is FC or ZFC. Meanwhile, the peak intensity is enhanced at high field without broadening as shown in Fig. 2**b** and Fig. S3. Such a magnetic maximum is usually observed in an AFM correlation dominated ordering. Tentatively, the transition temperature corresponding to the magnetic maximum is called as T_N a Neel temperature, since an AFM ordering is well accepted for a bipartite system at half-filling as in finite graphene fragments[1]. It is found the T_N value changed little (about 4 K) under fields varied from 1 to 30 kOe as shown in Fig. S3(c).

With lowering temperature further, an up turn appeared in M(T)/H curves at about 10 K at a 3 kOe field and about 40 K at 1 kOe field, no matter the process was FC or ZFC. A slight up turn of magnetic moment at low temperature was weakly exhibited in carbon nanotube (CNT)[24]. The up turn of magnetic moment at low temperature is critically related to the unequal numbers of the zigzag edges belonging to the two sublattices and the enlarged spin correlation length of a continuous zigzag edge which had been predicted to grow exponentially with decreasing temperature below 10 K[3]. The net magnetic moment contributed from the two sublattices is corresponding to a FM contribution whose moment is increased with lowering temperature due to an exponential enlargement of the spin correlation length resulted in an enlarged moment of a fundamental magnetic order unit (FMOU), which is defined as a continuous ferromagnetic coupled zigzag edges, and also a unit of net magnetic moment.

The DM susceptibility observed here can be quantitatively described by the Kotosonov's equation[21] developed from the first calculation of the conduction electron magnetic susceptibility in graphite by McClure[23]. The Kotosonov's equation is expressed as:

$$\chi = \frac{-1.46\times10^{-3} r_0^2}{T+\Delta T}\,\mathrm{sech}^2\left(\frac{E_F}{2k_B(T+\Delta T)}\right)\ (emu/g) \qquad (1)$$

Where r_0 is the band parameter in eV, E_F is Fermi energy, k_B is the Boltzmann constant, T is the temperature in degree Kelvin and ΔT is the degeneracy temperature $\Delta T = h/(2\pi^2 k_B \tau)$ (Dingle temperature) representing the energy broadening, where τ is the relaxation time for carriers and h is Planck constant. To fit the DM susceptibility at high temperature under 10 kOe field in the Fig. S4, the r_0, E_F and ΔT are taken as adjustable parameters to match the experimental data. If the r_0, E_F and ΔT are taken as 2.0 (1.7) eV, −5.4 (−6.8) meV and 65 K for the field perpendicular (parallel) to the GBPs, the high field

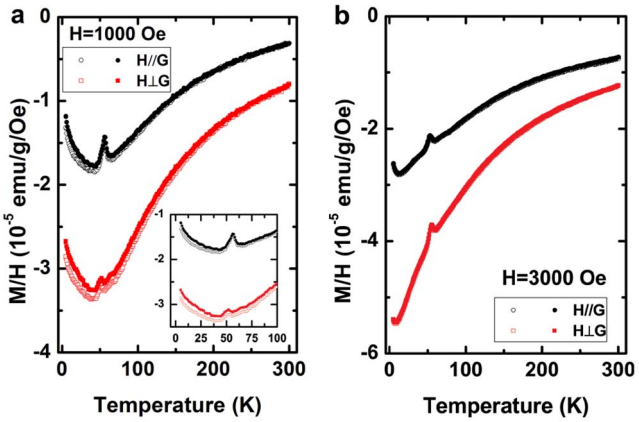

Figure 2 | Anisotropic magnetizations of the unidirectional aligned graphene sample as a function of temperature. The red (black) curve is corresponding to the applied field perpendicular (parallel) to the GBPs. The Fig. 2a and 2b are magnetization under 1 and 3 kOe fields at ZFC (opened symbols) and FC (filled symbols). The inset in Fig. 2a is a magnified magnetization around 50 K, indicating a divergence of magnetization under FC and ZFC.

DM susceptibilities can be well described by the Kotosonov's equation as drawn in Fig. S4. The Fermi energy of 5.4 to 6.5 meV is corresponding to a carrier degeneracy temperature E_F/k_B about 62 to 75 K, which is comparable to the deduced Dingle temperature 65 K mentioned above. And the deduced carrier relaxation time is about 38 *fs* corresponding to a carrier mean free path about 38 nm if a 10^6 m/s carrier speed is supposed. The short carrier free path in the studied graphene sheets is predominantly limited by the lateral size of the graphene sheets or a perfect graphene region in a graphene sheet where carbon atomic vacancies or macroscopic holes in the graphene sheet isolated the perfect graphene regions.

The anisotropic isothermal magnetization of the graphene sample as a function of applied field in range of −10 kOe to 10 kOe was measured at several different temperatures for the fields perpendicular and parallel to the GBPs respectively. M(H) curves at 10, 30, 50, 75, 100 and 200 K as representatives are shown in Fig. 3a to Fig. 3f after subtraction of their DM background. The used DM susceptibilities were marked in Fig. S4, matched well with the DM background described by the Kotosonov's equation.

M(H) curves shown in Fig. 3 reveal unusual magnetic ordering phenomena in three temperature ranges: T_I range lower than the T_N corresponding to Fig. 3**a** and 3**b**, T_{II} range around T_N shown in Fig. 3**c** and T_{III} range far higher than T_N as shown in Fig. 3**d**–3**f**. Figure 3**a**, as an example of T_I range, shows three magnetization regimes with increasing field: monotonically increased magnetic moment to a maximum at about 1–1.2 kOe for field perpendicular and parallel to the GBPs, then a slowly decreasing to a minimum at around 2.2 kOe, followed by a monotonously increasing with the applied field. Meanwhile, a weak coercive field about 100 Oe existed as seen in the inset of lower right of Fig. 3**a**. That means an anisotropic long range magnetic ordering existed in the sample. Because this temperature range is lower than the Neel temperature T_N, an AFM ordering should be reasonable. The unusual magnetic moment variation with field suggests there are at least three magnetic order phases existed in the present case. One is an AFM of the FMOUs belonging to different sublattices at field lower 3 kOe, who behaves like FM since the magnetic moments contributed by the FMOUs belonging to different sublattices are unequal. So, the net magnetic moment behaves like FM[1,25]. The second is possibly a superconductivity phase embodied in the graphene sheets, whose magnetic shield makes the total magnetic moment reduced with field increasing while the field is less than 4 kOe. The summation of the magnetic

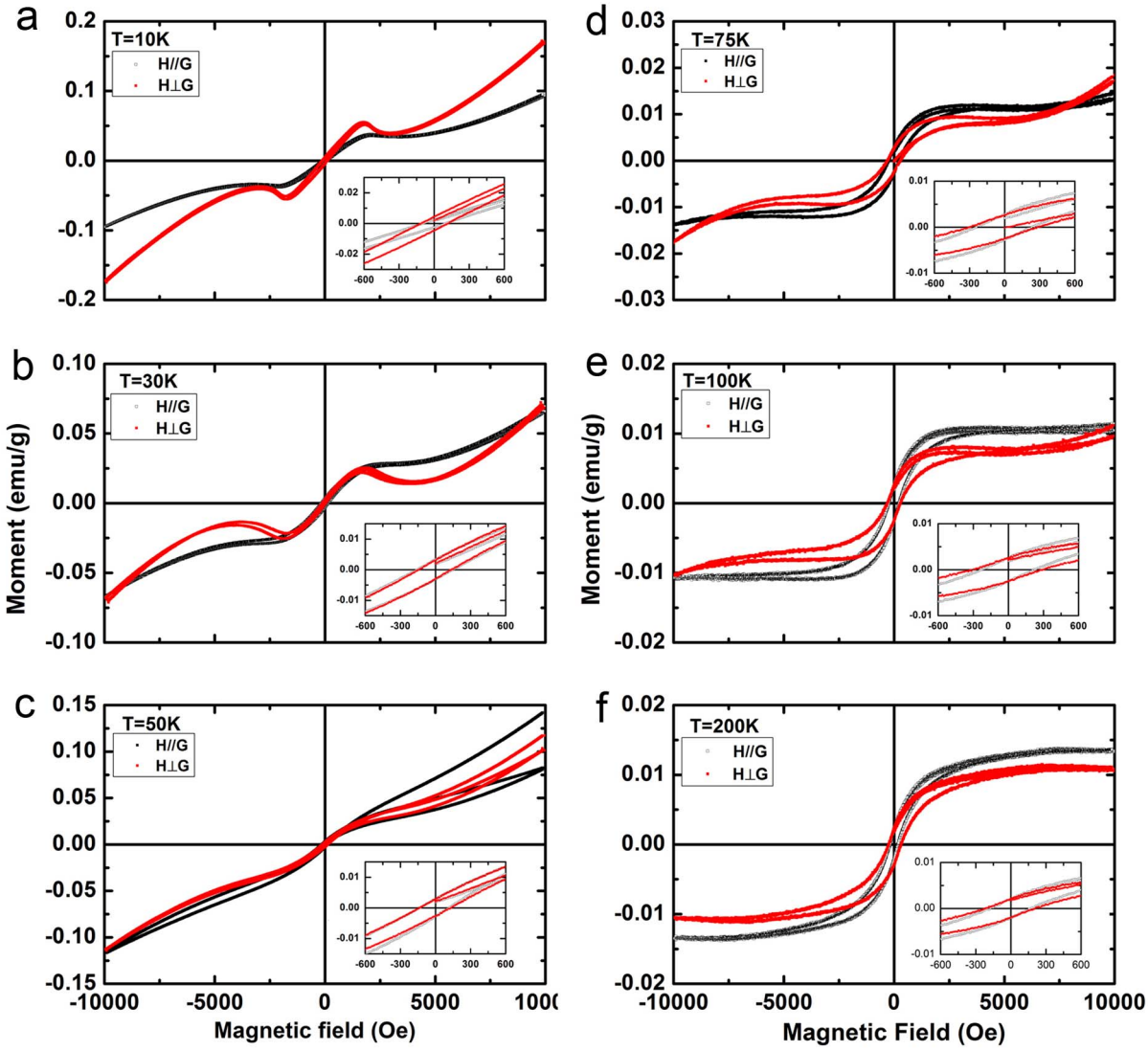

Figure 3 | Anisotropic isothermal magnetizations of the graphene sample at several representative temperatures with field perpendicular (red curves) or parallel (black curves) to the GBPs. The insets are magnified magnetization at low field to observe the coercive field clearly. Figure 3a to 3f are corresponding to 10, 30, 50, 75, 100 and 200 K in sequence.

moments of the AFM and the superconductivity shield can well reproduce the unusual magnetization. The third is a spin flip towards parallel FM alignments favored for the FMOUs belonging to different sublattices under an even higher field, because the strong interaction between the field and the magnetic moment suppresses the AFM super-exchange interaction of the FMOUs located at different sublattices. In T_I range, the ordering degree of the spin flip towards parallel alignment was gradually increased with the field becoming large.

In T_{II} range, the non-convergent hysteretic trajectories are found obviously as shown in Fig. 3**c**, and it is even prominent in the case of the fields parallel to the GBPs. The non-convergent hysteretic trajectories were predicted by Friedman and coworker[26] in a random binary antiferromagnetic coupled spin network. They suggested the phenomena are associated with the presence of specific topological elements in a network structure, particularly with the fully interconnected spin groups equal to or greater than 4. The theoretical prediction is exactly coincidence with our case, where the FMOU on the graphene edges is predicted to be at least 3–4 zigzag edges in a spin unit for FM ordering[27], which is comparable to the necessary numbers of the topological elements mentioned above. It is noted the unclosed hysteretic loops were also discernible at even higher temperatures as seen in Fig. 3**d** and 3**e**. However, the most serious case was found around the T_N, indicating that the competition between a long range AFM order of the FMOUs belonging to different sublattices and a thermal induced disorder of the FMOUs enhances the non-convergence of the hysteretic loop. A further experimental study on the dynamics of the non-convergent hysteretic phenomena is underway.

At high temperatures as shown in Fig. 3**d** to Fig. 3**f**, the magnetization is reduced to about 1/2 ~ 1/3 in low field and about one order lower in high field compared with that at low temperature. Oppositely, even large coercive fields are observed, such as about 300 Oe at about 75 K as shown in the inset of Fig. 3**d**. The large coercive field and near saturated hysteretic loops indicate an anisotropic long range magnetic ordering existed, which is clearly distinguished from that observed at low temperature. Therefore, it is inferred a FM ordering of the neighbored FMOUs through super-exchange interaction between them assisted by the itinerant carriers, whose free path was about 38 nm deduced above. However, the smaller saturation magnetization at high temperature is considered resulted from a decreased magnetic correlation length with increasing temperature, which was predicted to be inversely proportional to the temperature i. e. 300 nm/T for the temperature above 10 K[3].

Observing the insets of the magnified magnetization at low fields in Fig. 3**a** to Fig. 3**f**, it is noted the coercive fields were varied with temperature. Its variation versus temperature is shown in Fig. 4 exhibiting a ridge shaped variation with a maximum point at about 75 K and an abnormal variation point at about 50 K. The opposite variation trends of the coercive fields with temperature at two sides of lower 50 K and above 75 K suggests the magnetic ordering is different between the two temperature ranges. The distinguished orders should be corresponding to an AFM and a FM orderings, respectively. The inference is consistent with the analysis on Fig. 3. In framework of the Neel relaxation and the Bean-Livingston criteria, the coercive field of an assembly of non-interaction single-domain magnetic units with uniaxial anisotropy is expected to decay with the square root of temperature[28,29]. According to the relationship, the coercive fields of FM ordering were fitted for $T \geq 75$ K, and the deduced blocking temperature T_B, corresponding to a transition temperature from FM to super-PM, is about 820 ± 80 K for field perpendicular and parallel to the GBPs respectively. At the deduced blocking temperature, the spin correlation length is about 0.3 nm (only 2 zigzag edges contained), which is also a limit to start losing local FM correlation of the adjacent zigzag edges. The limit is consistent with a theoretical prediction on lower limit for generation of local magnetism of zigzag edges[27]. The coincidence of our experiment findings with theoretical prediction supports sufficiently the observed FM order of the FMOUs are contributed from the zigzag edges but not from contamination of some kinds of magnetic impurities as suspected in other graphene materials[2]. The so high FM order temperature suggests the magnetic order contributed by the graphene edge states is potential for high temperature spintronics.

Discussion

A quantitative description of magnetization behavior at RT in the field perpendicular to the GBPs, as an example, was given and shown in Fig. 5. The RT magnetization can be approximately described by the Brillouin function of a FM ordering system[30],

$$M = Ng_f J\mu_B \left[\frac{2J+1}{2J}\,\mathrm{ctnh}\left(\frac{(2J+1)x}{2J}\right) - \frac{1}{2J}\,\mathrm{ctnh}\left(\frac{x}{2J}\right)\right] \qquad (2)$$

Where $x = \dfrac{g_f J\mu_B H_e}{k_B T}$ is the ratio of the Zeeman energy of the magnetic moment in the effective field H_e to the thermal energy, the effective field $H_e = H + H_m$, where the H_m is the molecular field proportional to magnetic moment M, g_f is the g-factor, J the angular momentum

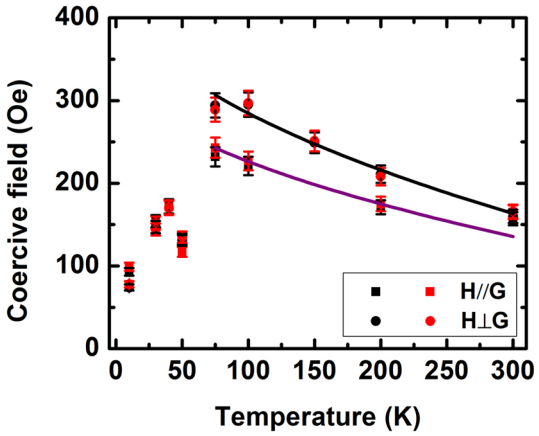

Figure 4 | Variation of coercive field with temperature for field perpendicular (circle symbols) and parallel (square symbols) to the GBPs. The black and red symbols express the negative and positive coercive fields respectively. The solid black (purple) line is a Bean-Livingston model fitting to the coercive field.

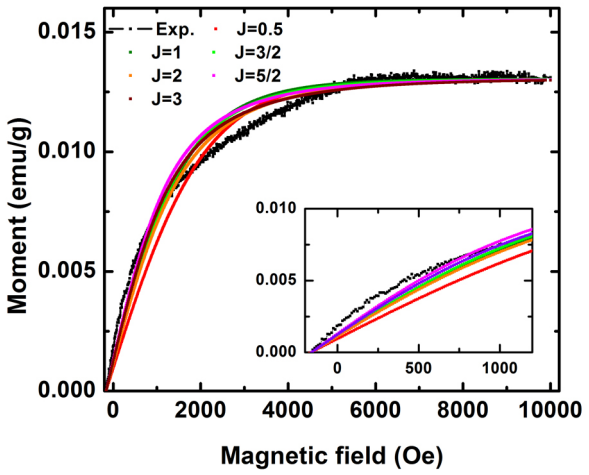

Figure 5 | Ferromagnetic Brillouin function fitting to the room temperature magnetization (black curves) of the graphene sheets with field perpendicular to the GBPs. The curves drawn by the color symbols were fitted to the magnetization with J = 0.5 to 3, respectively.

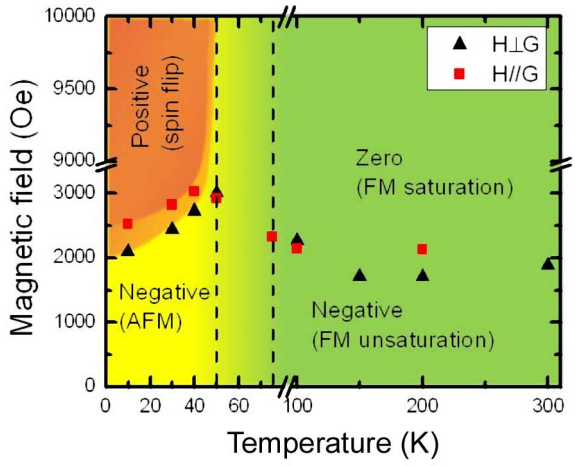

Figure 6 | Magnetic phase diagram of the graphene sheets with irregular zigzag edges. The light yellow, orange and green colors are corresponding to antiferromagnetic, spin flip and ferromagnetic ordering regions, respectively. The area in the dashed lines is a transition buffer region from AFM to FM orders. The filled black triangle and red square symbols express the sign transition points of the second order differential $d^2M(H)/dH^2$ of the raw isothermal magnetization versus the field for the field perpendicular and parallel to the GBPs, respectively.

number, N the number of spins, k_B the Boltzmann constant. To simplify the analysis, the effective field H_e is supposed to be proportional to the external field H, written as $H_e = \alpha(H - H_c)$, where α is a proportional constant closely related to the molecular field, and H_c is the coercive field at certain temperature (at 300 K, $H_c = -160$ Oe). Assuming $g_f = 2$, the Brillouin functions at FM ordering are described in Fig. 5 with the $J = 0.5$ to 3, $N = 1.4 \times 10^{18}/2$ J g^{-1} and α among $1.6 \pm 0.4 \times 10^3$. The large constant α means a strong molecular field. It is deduced the molecular field $H_m \approx \alpha(H - H_c)$, which is approximately over 1000 times of the applied field.

It is noted the $J = 5/2$ and 3 are better fitted to the magnetization in low and high fields at 300 K. If taken $J = 5/2$, it is inferred the spin number N is about 2.8×10^{17} g^{-1}, that is about one order smaller compared with that deduced in graphene nanocrystals reported by Geim and coworker[13]. The magnetization at RT allows us to infer that observed FM ordering is contributed from the FMOUs with an average moment $\mu = g_f J \mu_B \approx 5 \sim 6\ \mu_B$ in concentration about 5.6 ppm, indicating the continuous zigzag edges is at least $5 \sim 6$ zigzag units in length about $1 \sim 1.2$ nm, which is completely same to the theoretical predicted long range magnetic order correlation length 1 nm at RT[3]. The coincidence of experimental observation and theoretical prediction in magnetic moment of a FMOU at RT provides a favorable aspect to support the magnetism coming from the zigzag edges. In addition, if the molecular field inducing the FM interaction of the FMOUs is imaged as a external field, the interaction energy of a moment with the field can be expressed as $\mu H_m = g_f J \mu_B H_m$, that is approximately equivalent to a thermal energy at temperature about 1000 K, as if taken a applied external field $H = 3$ kOe at which magnetization is tending to saturation as shown in Fig. 5. The temperature deduced here is corresponding to a FM Curie temperature and is comparable to the blocking temperature deduced above. The consistence of the both temperatures further supports the point of view of the observed magnetism coming from the FMOUs located at zigzag edges of the graphene sheets.

Based on the experimental results above and rational analysis, a magnetic phase diagram of the FMOUs is constructed first time in the temperature and magnetic field scheme as shown in Fig. 6. It is noted three magnetic ordering phases and a transition region existed for the FMOUs, 1) an AFM at low temperature and low magnetic field region marked by the light yellow color in Fig. 6, where the FMOUs posses a relative long correlation length. The FMOUs belonging to the same sublattice behave like similar FM units, but the FMOUs belonging to different sublattices in the same graphene sheet tend to anti-parallel alignment; 2) a spin flip phase at low temperature and a higher field region marked by the orange color in Fig. 6, where interaction of the FMOUs and the magnetic field is strong enough to destroy the AFM ordering of the FMOUs belonging to different sublattices to flip the spins towards the field; 3) a short range FM ordering is prevailed for the FMOUs at high temperature over 75 K marked by green color in Fig. 6, where the total magnetic moment is near one order reduced compared with that at 10 K. Two possible reasons dominated the reduced magnetization. One is the reduced spin correlation length at high temperature. The other is a short carrier mean free path at high temperature renders a short range magnetic ordering of the FMOUs. 4) a transition buffer region from the AFM to the FM inside the two dashed lines, due to a competition of AFM interaction and thermal induced disorder.

The deduced magnetic phase diagram is supported sufficiently by the second order differential $d^2M(H)/dH^2$ of the isothermal magnetization versus the magnetic field at a given temperature as shown in Fig. 6 marked with the scattering symbols. The first order differential dM(H)/dH of the isothermal magnetization versus the field at different temperature is shown in Fig. S6. The sign of the $d^2M(H)/dH^2$ under a frame of the field and temperature is summarized in Fig. 6. The boundary of the sign change is marked by the filled black triangle and red square symbols for the field perpendicular and parallel to the GBPs respectively. The regions represented by the signs of positive and zero are corresponding to spin flip and FM saturation regimes respectively. While, the region marked with negative includes two regimes. They are AFM phase at temperature lower 50 K and unsaturated FM phase at temperature higher 75 K, respectively. The magnetic phase diagram is helpful to understand the experimental results reported here intuitively and clarify the controversial magnetic phenomena reported early. If the FMOUs contained more than three zigzag edges, ferromagnetism would be observed at room temperature, otherwise paramagnetism. Significantly, it provides a clear physics of magnetic interactions of the FMOUs located at the zigzag edges in graphene, and contributed a deeper insight into the nature of magnetism in graphene based system and even recasts a possibility towards graphene spintronics.

Methods

The graphene sample was fabricated by high temperature over 1700°C annealing SiC (10-10) slices in thickness about 400 μm for over 6 hrs under a vacuum ambient with a pressure about 10^{-2} Pa. The Si atoms were completely sublimated from the SiC slice and C atoms remained only reconstructed into graphene sheet assemblage with unidirectional alignment of the graphene basal planesas in height about 391 μm. The layer number of each graphene sheet is about several to some dozens of monolayer as analyzed by TEM in Fig. S1. The Raman scattering, scanning electron microscopy (SEM), transmission electron microscopy (TEM), X-ray photoelectron spectroscopy (XPS) and electron spin resonant (ESR) were employed to characterize the sample. The DC-magnetization measurements as a function of temperature (T) or magnetic field (H) were carried out using a Quantum Design PPMS-9 magnetometer and a Vibrating Sample Magnetometer (VSM), respectively. The temperature dependent magnetization M(T) curves for all samples were recorded in the warming cycle over the temperature range of 10 (partly from 5 K) to 300 K in ZFC and FC conditions. The field dependent magnetization M(H) curves over all four quadrants (including the initial leg) were recorded at 10 to 300 K under a maximum magnetic field 10 kOe. For the M(H) measurement, the sample was first cooled down from room temperature to a target temperature under a ZFC condition.

1. Yazyev, O. V. Emergence of magnetism in graphene materials and nanostructures. *Rep Prog Phys* **73**, 056501 (2010).
2. Nair, R. R. *et al.* Spin-half paramagnetism in graphene induced by point defects. *Nat Phys* **8**, 199–202 (2012).
3. Yazyev, O. V. & Katsnelson, M. I. Magnetic correlations at graphene edges: Basis for novel spintronics devices. *Phys Rev Lett* **100**, 047209 (2008).
4. Soriano, D., Munoz-Rojas, F., Fernandez-Rossier, J. & Palacios, J. J. Hydrogenated graphene nanoribbons for spintronics. *Phys Rev B* **81**, 165409 (2010).

5. Joly, V. L. J. *et al*. Effect of electron localization on the edge-state spins in a disordered network of nanographene sheets. *Phys Rev B* **81**, 115408 (2010).
6. Yazyev, O. V. & Helm, L. Defect-induced magnetism in graphene. *Phys Rev B* **75**, 125408 (2007).
7. Jung, J., Pereg-Barnea, T. & MacDonald, A. H. Theory of Interedge Superexchange in Zigzag Edge Magnetism. *Phys Rev Lett* **102**, 227205 (2009).
8. Fujita, M., Wakabayashi, K., Nakada, K. & Kusakabe, K. Peculiar localized state at zigzag graphite edge. *J Phys Soc Jpn* **65**, 1920–1923 (1996).
9. Ma, Y. C., Lehtinen, P. O., Foster, A. S. & Nieminen, R. M. Magnetic properties of vacancies in graphene and single-walled carbon nanotubes. *New Journal of Physics* **6**, 68 (2004).
10. Cervenka, J., Katsnelson, M. I. & Flipse, C. F. J. Room-temperature ferromagnetism in graphite driven by two-dimensional networks of point defects. *Nat Phys* **5**, 840–844 (2009).
11. Wang, Y. *et al*. Room-Temperature Ferromagnetism of Graphene. *Nano Lett* **9**, 220–224 (2009).
12. Rao, S. S. *et al*. Ferromagnetism in Graphene Nanoribbons: Split versus Oxidative Unzipped Ribbons. *Nano Lett* **12**, 1210–1217 (2012).
13. Sepioni, M. *et al*. Limits on Intrinsic Magnetism in Graphene. *Phys Rev Lett* **105**, 207205 (2010).
14. Scheike, T. *et al*. Can Doping Graphite Trigger Room Temperature Superconductivity? Evidence for Granular High-Temperature Superconductivity in Water-Treated Graphite Powder. *Adv Mater* **24**, 5826–5831 (2012).
15. Lin, Y. M. *et al*. 100-GHz Transistors from Wafer-Scale Epitaxial Graphene. *Science* **327**, 662–662 (2010).
16. Huang, Q. S. *et al*. Approaching the Intrinsic Electron Field-Emission of a Graphene Film Consisting of Quasi-Freestanding Graphene Strips. *Small* **7**, 450–454 (2011).
17. Chen, L. L., Guo, L. W., Wu, Y., Jia, Y. P. & Li, Z. L. Fabrication of vertically aligned graphene sheets on SiC substrates. *RSC Adv* (2013).
18. Li, X., Magnuson, C. W., Venugopal, A., Tromp, R. M., Hannon, J. B., Vogel, E. M. *et al*. Large-Area Graphene Single Crystals Grown by Low-Pressure Chemical Vapor Deposition of Methane on Copper. *J Am Chem Soc* **133**, 2816–2819 (2011).
19. Li, X. S., Cai, W. W., Colombo, L. & Ruoff, R. S. Evolution of Graphene Growth on Ni and Cu by Carbon Isotope Labeling. *Nano Lett* **9**, 4268–4272 (2009).
20. Krishnan, K. S. & Ganguli, N. Temperature Variation of the Abnormal Unidirectional Diamagnetism of Graphite Crystals. *Nature* **139**, 155 (1937).
21. Kotosonov, A. S. Diamagnetism of quasi-two-dimensional graphites. *Jetp Lett* **43**, 37–40 (1986).
22. Ganguli, N. & Krishnan, K. S. The magnetic and other properties of the free electrons in graphite. *Proc R Soc Lond A* **177**, 168–182 (1941).
23. McClure, J. W. Diamagnetism of graphite. *Phys Rev* **104**, 666–671 (1956).
24. Heremans, J., Olk, C. H. & Morelli, D. T. Magnetic-susceptibility of carbon structures. *Phys Rev B* **49**, 15122–15125 (1994).
25. Lieb, E. H. Two theorems on the Hubbard model. *PhysRevLett* **62**, 1201–1204 (1989).
26. Hovorka, O. & Friedman, G. Nonconverging hysteresis cycles in random spin networks. *Phys Rev Lett* **100**, 097201 (2008).
27. Kumazaki, H. & Hirashima, D. S. Local magnetic moment formation on edges of graphene. *J Phys Soc Jpn* **77**, 044705 (2008).
28. Bean, C. P. & Livingston, J. D. Superparamagnetism. *J Appl Phys* **30**, 120s–129s (1959).
29. Nunes, W. C., Folly, W. S. D., Sinnecker, J. P. & Novak, M. A. Temperature dependence of the coercive field in single-domain particle systems. *Phys Rev B* **70**, 014419 (2004).
30. Kittel, C. *Introduction to Solid State Physics*, 8th edn: New York 1996.

Acknowledgements

This work is partly supported by the ministry of science and technology of china (grant No. 2011CB932700), the Knowledge Innovation Project of Chinese Academy of Science (grant No. KJCX2-YW-W22), and the national science foundation of china (grant Nos. 51272279 and 51072223).

Author contributions

L.W.G. designed the experimental scheme and analyzed the experimental data. L.L.C. did the most of the sample preparation and characterizations. L.W.G. and X.L.C. wrote and revised the manuscript. Z.L.L. did the part of work in model fitting. H.Z., J.J.L., J.H. and S.F.J. helped with the experiment. All authors reviewed this manuscript.

Additional information

Supplementary information accompanies this paper at http://www.nature.com/scientificreports

Competing financial interests: The authors declare no competing financial interests.

How to cite this article: Chen, L. *et al*. Towards intrinsic magnetism of graphene sheets with irregular zigzag edges. *Sci. Rep.* **3**, 2599; DOI:10.1038/srep02599 (2013).